View metadata, citation and similar papers at core.ac.uk

brought to you by CORE

provided by NASA Technical Reports Server

Old Dominion University Research Foundation

DEPARTMENT OF MECHANICAL ENGINEERING AND MECHANICS
COLLEGE OF ENGINEERING AND TECHNOLOGY
OLD DOMINION UNIVERSITY
NORFOLK, VIRGINIA 23529

LANGLEY
GRANT
NN-54-CR
150134
P-29

LARGE PLANAR MANEUVERS FOR ARTICULATED FLEXIBLE MANIPULATORS

By

Jen-Kuang Huang, Principal Investigator

and

Li-Farn Yang

Progress Report
For the period ended May 31, 1988

Prepared for the
National Aeronautics and Space Administration
Langley Research Center
Hampton, Virginia 23665

Under
Research Grant NAG-1-830
Dr. Jer-Nan Juang, Technical Monitor
SDD-Structural Dynamics Branch

(NASA-CR-183079) LARGE PLANAR MANEUVERS FOR ARTICULATED FLEXIBLE MANIPULATORS Progress Report, period ended 31 May 1988 (Old Dominion Univ.) 29 p CSCL 05H

N88-26104

Unclas
G3/54 0150134

July 1988

DEPARTMENT OF MECHANICAL ENGINEERING AND MECHANICS
COLLEGE OF ENGINEERING AND TECHNOLOGY
OLD DOMINION UNIVERSITY
NORFOLK, VIRGINIA 23529

LARGE PLANAR MANEUVERS FOR ARTICULATED FLEXIBLE MANIPULATORS

By

Jen-Kuang Huang, Principal Investigator

and

Li-Farn Yang

Progress Report
For the period ended May 31, 1988

Prepared for the
National Aeronautics and Space Administration
Langley Research Center
Hampton, Virginia 23665

Under
Research Grant NAG-1-830
Dr. Jer-Nan Juang, Technical Monitor
SDD-Structural Dynamics Branch

Submitted by the
Old Dominion University Research Foundation
P. O. Box 6369
Norfolk, Virginia 23508-0369

July 1988

Large Planar Maneuvers for Articulated Flexible Manipulators

Jen-Kuang Huang and Li-Farn Yang
Dept. of Mechanical Engineering and Mechanics
Old Dominion University
Norfolk, Virginia 23508

Jer-Nan Juang
Mail Stop 230
NASA Langley Research Center
Hampton, Virginia 23665

Abstract

An articulated flexible manipulator carried on a translational cart is maneuvered by an active controller to perform certain position control tasks. The nonlinear dynamics of the articulated flexible manipulator are derived and a transformation matrix is formulated to localize the nonlinearities within the inertia matrix. Then a feedback linearization scheme is introduced to linearize the dynamic equations for controller design. Through a pole placement technique, a robust controller design is obtained by properly assigning a set of closed-loop desired eigenvalues to meet performance requirements. Numerical simulations for the articulated flexible manipulators are given to demonstrate the feasibility and effectiveness of the proposed position control algorithms.

Introduction

Research and experiments on control of large flexible manipulators have gained much attention in the past decade. The merits of flexible manipulators over rigid ones are light weight and small power consumption. However, the trade-off is in developing a feasible control scheme not only to effectively accomplish the assigned task, but also to minimize the flexible vibrations. Several investigators have studied the dynamics and control of the flexible manipulators [1-6]. Most flexible manipulators are composed of one or, at most, two flexible beam-like arms rotated by the actuators in planar motion. The nonlinear characteristics of the dynamic models are either linearized or eliminated due to their relatively small contributions. Nevertheless, the behavior due to dynamic nonlinearities becomes significant under quick maneuvers or large motions. Investigation into dynamic nonlinearities provides a very useful way for the feasible control design of the large flexible manipulators.

In this paper, an articulated flexible manipulator is studied. The system consists of a rigid translational cart with one flexible beam-like arm attached on a motor at one end, and an equivalent arm hinged on the tip at the other end. Two motors are concatenated axially upon the cart. The additional motor

transmits the torque to the elbow joint through a wire to manipulate the forearm. This appendage expands the workspace wherein which the tip of the articulated manipulator can reach. It also develops another degree of freedom associated with the rigid body. Two kinds of interactions of kinematic nonlinearities appear significantly [7]. One is introduced through the coupling of the rigid cart and the flexible arms. The other takes place due to the interaction of the two articulated flexible arms.

The dynamics equations are derived using Lagrange's equations of motion along with classical vibration theory [8-10]. Actuator dynamics are briefly described and are included in the system equations to complete the dynamic model of the system [11]. Nonlinearities in the inertia matrix are localized using an appropriate transformation matrix and are linearized using a feedback linearization scheme [7,12,13]. A robust pole placement method [14] is then applied to obtain a well-conditioned output feedback controller so that closed-loop eigenvalues are insensitive to system uncertainties or perturbations. Several simulations are given to illustrate the feasibility and effectiveness of active position control schemes in performing translational and slewing tasks while suppressing flexural vibrations of each flexible arm.

System Dynamics

For the sake of clarity and simplicity, this section begins with the derivation of one-arm manipulator dynamics, then is followed by the dynamic model formulation for the articulated manipulators.

a. One-arm Manipulator Dynamics:

In Fig. 1, the single planar flexible arm is clamped on the axial shaft of the motor by a hinge. This motor is mounted on a translational cart which is driven along a linear track by another motor. The beam-like flexible arm is modeled as a cantilever beam with the fixed end at the motor and the free end at the tip x_1=L. Only the bending vibration is allowed during the motion of the arm. The x-y axes are the fixed inertial coordinate, whereas, the x_1-y_1 axes represent the moving relative coordinate. Lagrange's equation of motion, in conjuction with the modal expansion to discretize the deflection of the flexible manipulators, is applied to derive the dynamic equations of motion. Denote EI the bending rigidity, ρ the mass density of the arm per unit length, L the length of the flexible arm, and M the total mass of the cart and the arm driver. Let the state vector be defined by

$$\xi = (y, \theta_1, q_1^T)^T \quad ; q_1^T = (q_{11}, q_{12}, \ldots\ldots, q_{1n_1}) \tag{1}$$

ORIGINAL PAGE IS
OF POOR QUALITY

where y is the translational displacement of the cart, θ_1 the root angle of the flexible arm, and q_{1i} $(i=1,\ldots,n_1)$ the general coordinates corresponding to the shape functions ψ_{1i} $(i=1,\ldots,n_1)$ for discretization of the bending deflection of the flexible arm. The control torques introduced by the two motors can be expressed by the vector

$$\tau = (\tau_0 , \tau_1 , 0, \ldots, 0)^T \qquad (2)$$

where τ_0 and τ_1 represent the applied torques for the cart and the flexible arm respectively.

The equations of motion including actuator dynamics can then be written by

$$M\ddot{\xi} + K\xi = f(\xi,\dot{\xi}) + \tau \qquad (3)$$

in which the inertia matrix reads

$$M = \begin{bmatrix} m + \rho L & & \textbf{Symmetric} \\ \rho L^2 c\theta_1/2 & I_1 & \\ -h_1 c\theta_1 & -P_1 & \rho L\, \hat{I}_1 \end{bmatrix} \qquad (4)$$

where the superscript T in $(\ )^T$ means the transpose of the matrix $(\ )$, $\hat{I}_1$ is an $n_1 \times n_1$ identity matrix, and $c\theta_1 = \cos(\theta_1)$. The constant vectors h_1 and P_1 are defined in the appendix which also shows the detailed derivation of equation (3). The constant stiffness matrix shows

$$K = \text{Diag}\ [\ 0,\ 0,\ \rho L\omega_1^2\ ] \qquad ;\ \omega_1 = \text{Diag}\ [\ \omega_{11}, \ldots,\ \omega_{1n_1}\ ] \qquad (5)$$

where ω_{1i} $(i=1,\ldots,n_1)$ are the frequencies associated with the shape functions $\psi_{1i}(x_1)$, which are used to discretize the deflection of the flexible arm. The nonlinear force yields

$$f(\xi,\dot{\xi}) = \begin{bmatrix} s\theta_1(\rho L^2\dot{\theta}_1^2/2 - h_1^T\dot{q}_1\dot{\theta}_1) \\ s\theta_1 h_1^T\dot{q}_1\dot{y} \\ -s\theta_1 h_1\dot{\theta}_1\dot{y} \end{bmatrix} \qquad (6)$$

where $s\theta_1 = \sin(\theta_1)$.

The actuator dynamics and sensor characteristics play major roles in the controller design. The two actuators for the feedback control are dc electric motors. The electric motor can be regarded as a standard armature circuit. Denote the armature resistance by R_a, the back-EMF (Electro-Motive-Force) constant by K_b, the motor torque constant by K_t, the gear train viscous drag coefficient by C_v , the motor inertia by I_m, and the overall gear ratio by N_g. Then the torque τ produced by the actuator provides [11]

$$\tau = (N_g K_t/R_a)e_a - (K_t K_b/R_a + C_v)N_g^2\dot{\theta} - I_m N_g^2\theta \qquad (7)$$

where e_a is the applied voltage into the armature and θ is the output shaft angle θ_1. Note that θ in equation (7) is identical to the root angle of the flexible arm. For the case of the translational cart, it is equivalent to the linear displacement y divided by the transmission pulley radius r. Apparently, the passive damping of the whole system results from the second term in equation (7).

Referring to the sensors, the rotational angles are measured by the 10-turn rotary potentiometers, whereas, the angular velocities are calibrated by the tachometers. Strain gages are used to sense the bending moments along the flexible arm. Denote c_p the conversion factor between the output shaft angle and the output voltage e_p of the potentiometer, c_t the conversion factor between the output angular velocity and the output voltage e_t, c_s the conversion factor between the strain and the strain output voltage e_o. Suppose two strain gages are placed along the flexible arm respectively at x_1 and x_2 as shown in Fig. 2a. An output measurement equation can be written in the following matrix form

$$\hat{e} = [e_{t_0}, e_{t_1}, e_{p_0}, e_{p_1}, e_o(x_1), e_o(x_2)]^T = C_f [\dot{y}, \dot{\theta}_1, \xi^T]^T \qquad (8)$$

$$= \mathrm{Diag}[c_{t_0}/r, c_{t_1}, c_{p_0}/r, c_{p_1}, C_\varepsilon][\dot{y}, \dot{\theta}_1, y, \theta_1, q_1^T]^T$$

where

$$C_\varepsilon = c_s h \begin{bmatrix} \psi_{1,xx}(x_1), \ldots, \psi_{n,xx}(x_1) \\ \psi_{1,xx}(x_2), \ldots, \psi_{n,xx}(x_2) \end{bmatrix},$$

$$\psi_{i,xx}(x_1) = \partial^2\psi_i(x)/\partial x^2\big|_{x=x_1},$$

$q_1 = [q_{11}, \ldots, q_{1n_1}]^T$ and h is the half-thickness of the flexible arm. Equation (8) relates the output voltage $\hat{e}$ to the state variables y, θ_1 and ξ through the coefficients of the matrix C_f.

Substituting equation (7) into equation (3) provides

$$\bar{M}\ddot{\xi} + \bar{C}\dot{\xi} + K\xi = BE_a(t) + f(\xi,\dot{\xi}) \tag{9}$$

in which,

$$\bar{M} = M + \text{Diag}\,[I_{m_0}N_{g_0}^2/r,\ I_{m_1}N_{g_1}^2,\ 0,\ 0]$$

$$\bar{C} = \text{Diag}\,[\ (K_{t_0}K_{b_0}/R_{a_0}+C_{v_0})N_{g_0}^2/r,\ (K_{t_1}K_{b_1}/R_{a_1}+C_{v_1})N_{g_1}^2,\ 0,\ 0\ ]$$

$$B = \begin{bmatrix} N_{g_0}K_{t_0}r/R_{a_0} & 0 \\ 0 & N_{g_1}K_{t_1}/R_{a_1} \\ 0 & 0 \\ 0 & 0 \end{bmatrix}$$

and $E_a(t)=(e_{a_0},e_{a_1})^T$ with e_{a_0} and e_{a_1} being the applied voltages for the motors of the cart and the flexible arm respectively.

b. Articulated Manipulator Dynamics:

In order to expand the workable region of the flexible manipulators, one beam-like flexible arm is articulated on the tip of the previous arm as shown in Fig. 3. This additional arm is also treated as a fixed-free cantilever beam. This system has three (one translational and two rotational) degrees of freedom attributed to rigid body motion. One more actuator is required, which concatenated axially with the former one on the rigid cart. The forearm is manipulated by this additional motor through a wire. In Fig. 3, the mass M includes the mass of the new motor for the forearm. Denote θ_1 the root angle of the first flexible arm and θ_2 the root angle of the forearm measured relative to the previous local coordinates, i.e., x_1-y_1 axes.

The state vector similar to equation (1) becomes

$$\xi=(y,\theta_1,\theta_2,q_1^T,q_2^T)^T \;;\; q_1^T=(q_{11},\ldots,q_{1n_1}) \text{ and } q_2^T=(q_{21},\ldots,q_{2n_2}) \qquad (10)$$

where y is the translational displacement of the cart and q_{1i} $(i=1,\ldots,n_1)$ the general coordinates corresponding to the shape functions ψ_{1i} $(i=1,\ldots,n_1)$ for discretization of the bending deflection of the first flexible arm. The quantities q_{2i} and ψ_{2i} are defined similarly for the forearm. The input vector for the articulated flexible arms is

$$\tau = (\tau_0,\tau_1,\tau_2,0,\ldots\ldots,0)^T \qquad (11)$$

where τ_0 represents the applied torque for the cart, and τ_1 and τ_2 for the two flexible arms.

Application of Lagrange's equations of motion in terms of state variables yields a set of equations in matrix form as equation (3). The symmetry inertia matrix becomes

$$M = \begin{bmatrix} m+2\rho L & & & & \\ 3\rho L^2 c\theta_1/2 & 4I_1 & & \text{Symmetric} & \\ \rho L^2 c(\theta_1+\theta_2)/2 & \rho L^3 c\theta_2/2 & I_2 & & \\ -h_1 c\theta_1 & -\rho L^2\psi_1(L) & -\rho L^2\psi_1(L)c\theta_2/2 & \rho L\psi_1(L)\psi_1^T(L) & \\ -\rho L\psi_1(L)c\theta_1 & -P_1 & & +\rho L\hat{I}_1 & \\ -h_2 c(\theta_1+\theta_2) & -Lh_2 c\theta_2 & -P_2 & h_2\psi_1^T(L)c\theta_2 & \rho L\hat{I}_2 \end{bmatrix} \qquad (12)$$

where $c\theta_1 = \cos(\theta_1)$, $c\theta_2 = \cos(\theta_2)$ and $c(\theta_1+\theta_2) = \cos(\theta_1+\theta_2)$. Here $\hat{I}_1$ and $\hat{I}_2$ are $n_1 \times n_1$ and $n_2 \times n_2$ identity matrices respectively with n_1 and n_2 being the numbers of the mode shapes respectively for discretization of bending deflections of the two beam-like flexible arms. Moreover, the stiffness matrix becomes

$$K=\text{Diag}[0,0,0,\rho L\omega_1^2,\rho L\omega_2^2]\;;\omega_1=\text{Diag}[\omega_{11},..,\omega_{1n_1}] \text{ and } \omega_2=\text{Diag}[\omega_{21},..,\omega_{2n_2}] \qquad (13)$$

and the nonlinear force vector is

$$f(\xi,\dot{\xi}) = (f_0, f_1, f_2, f_3, f_4)^T \tag{14}$$

where

$$f_0 = 3\rho L^2 s\theta_1 \dot{\theta}_1^2/2 - s\theta_1 (h_1^T \dot{q}_1)\dot{\theta}_1 - s(\theta_1+\theta_2)(h_2^T \dot{q}_2)(\dot{\theta}_1+\dot{\theta}_2)$$
$$+ \rho L^2 s(\theta_1+\theta_2)\dot{\theta}_2(\dot{\theta}_1+\dot{\theta}_2)/2 - \rho L s\theta_1 (\psi_1^T(L)\dot{q}_1)\dot{\theta}_1$$

$$f_1 = s\theta_1 (h_1^T \dot{q}_1)\dot{y} + s(\theta_1+\theta_2)(h_2^T \dot{q}_2)\dot{y} - \rho L^2 s(\theta_1+\theta_2)\dot{y}\dot{\theta}_2/2$$
$$+\rho L s\theta_1 (\psi_1^T(L)\dot{q}_1)\dot{y} + \rho L^3 s\theta_2 \dot{\theta}_2^2/2 - L s\theta_2 (h_2^T \dot{q}_2)\dot{\theta}_2$$

$$f_2 = s(\theta_1+\theta_2)(h_2^T \dot{q}_2)\dot{y} - s\theta_2 (\psi_1^T(L)\dot{q}_1)(h_2^T \dot{q}_2)$$
$$+ \rho L^2 s(\theta_1+\theta_2)\dot{y}\dot{\theta}_1/2 + L s\theta_2 (h_2^T \dot{q}_2)\dot{\theta}_1$$

$$f_3 = -s\theta_1 h_1 \dot{y}\dot{\theta}_1 - \rho L s\theta_1 \psi_1(L)\dot{y}\dot{\theta}_1 - \rho L^2 \psi_1(L) s\theta_2 \dot{\theta}_2^2/2$$
$$+ s\theta_2 \psi_1(L)(h_2^T \dot{q}_2)\dot{\theta}_2$$

$$f_4 = -h_2 s(\theta_1+\theta_2)\dot{y}(\dot{\theta}_1+\dot{\theta}_2) - L s\theta_2 h_2 \dot{\theta}_1\dot{\theta}_2$$
$$+ h_2 s\theta_2 (\psi_1^T(L)\dot{q}_1)\dot{\theta}_2$$

where $s\theta_1 = \sin(\theta_1)$, $s\theta_2 = \sin(\theta_2)$, and $s(\theta_1+\theta_2) = \sin(\theta_1+\theta_2)$.

Similar to equation (8), the output measurement equation is

$$\hat{e} = [e_{t_0}, e_{t_1}, e_{t_2}, e_{p_0}, e_{p_1}, e_{p_2}, e_{o_1}(x_1), e_{o_1}(x_2), e_{o_2}(x_1), e_{o_2}(x_2)]^T$$
$$= C_f[\dot{y}, \dot{\theta}_1, \dot{\theta}_2, \xi^T]^T \tag{15}$$

where

$$C_f = \mathrm{Diag}[c_{t_0}/r,\ c_{t_1},\ c_{t_1},\ c_{p_0}/r,\ c_{p_1},\ c_{p_1},\ C_{\varepsilon_1},\ C_{\varepsilon_2}]$$

$$C_{\varepsilon_i} = c_s h \begin{bmatrix} \psi_{i1,xx}(x_1), \ldots, \psi_{in_1,xx}(x_1) \\ \psi_{i1,xx}(x_2), \ldots, \psi_{in_2,xx}(x_2) \end{bmatrix} \quad \text{for } i = 1, 2$$

Similar to equation (9), the dynamic equations can be developed yielding

$$\bar{M} = M + \mathrm{Diag}[\ I_{m_0} N_{g_0}^2/r,\ I_{m_1} N_{g_1}^2,\ I_{m_1} N_{g_1}^2,\ 0,\ 0,\ 0,\ 0\ ] \tag{16}$$

$$\bar{C} = \mathrm{Diag}[(K_{t_0} K_{b_0}/R_{a_0} + C_{v_0}) N_{g_0}^2/r, (K_{t_1} K_{b_1}/R_{a_1} + C_{v_1}) N_{g_1}^2, (K_{t_1} K_{b_1}/R_{a_1} + C_{v_1}) N_{g_1}^2, 0, 0, 0, 0]$$

$$B = \begin{bmatrix} N_{g_0} K_{t_0} r/R_{a_0} & 0 & 0 \\ 0 & N_{g_1} K_{t_1}/R_{a_1} & 0 \\ 0 & 0 & N_{g_1} K_{t_1}/R_{a_1} \\ 0 & 0 & 0 \\ 0 & 0 & 0 \\ 0 & 0 & 0 \\ 0 & 0 & 0 \end{bmatrix}$$

and $E_a(t) = (e_{a_0}, e_{a_1}, e_{a_2})^T$

Feedback Linearization

To convert the equation of motion, equation (9), to the standard first-order state equations, the inertia matrix $\bar{M}$ must be inverted. In view of equations (9) and (16), it is seen that the matrix $\bar{M}$ is highly nonlinear and time variant, particularly for the articulated flexible manipulator. Direct inversion of the matrix $\bar{M}$ is impractical. An alternative approach is to seek a state variable transformation to localize the nonlinear terms to minimize the participation of the nonlinear terms in the matrix. Thus a state variable transformation is developed and written as

$$\xi(t) = \tilde{L}\eta(t) \tag{17}$$

where the transformation matrix $\tilde{L}$ for one-arm manipulator is:

$$\tilde{L} = \begin{bmatrix} 1 & 0 & 0 \\ 0 & 1 & h_1 \\ 0 & 0 & \rho L^2 \hat{I}_1/2 \end{bmatrix}$$

and for the articulated manipulator is

$$\tilde{L} = \begin{bmatrix} 1 & 0 & 0 & 0 & 0 & 0 \\ 0 & 1 & 0 & 3\rho L[h_{11}\Psi_{12}(L) - h_{12}\Psi_{11}(L)]/2 & 3\rho L[h_{11}\Psi_{12}(L) - h_{12}\Psi_{11}(L)]/2 & 0 \\ 0 & 0 & 1 & 0 & 0 & h_2 \\ 0 & 0 & 0 & 3\rho L^2[h_{12} - \rho L\Psi_{12}(L)/2]/2 & -3\rho L^2[h_{12} - \rho L\Psi_{12}(L)/2]/2 & 0 \\ 0 & 0 & 0 & -3\rho L^2(h_{11} - \rho L\Psi_{11}(L)/2]/2 & 3\rho L^2[h_{11} - \rho L\Psi_{11}(L)/2]/2 & 0 \\ 0 & 0 & 0 & 0 & 0 & \rho L^2 \hat{I}_2/2 \end{bmatrix}$$

in which only two mode shapes for each flexible arm are considered. Inserting equation (17) into equation (9) and premultiplying by $\tilde{L}^T$ yields

$$\tilde{M}\,\ddot{\eta} + \tilde{C}\,\dot{\eta} + \tilde{K}\,\eta = \tilde{L}^T B E_a + \tilde{L}^T f(\eta,\dot{\eta}) \tag{18}$$

where

$$\tilde{M} = \tilde{L}^T \bar{M} \tilde{L} = \begin{bmatrix} \tilde{M}_{00}(\eta,\dot{\eta}) & \tilde{M}_{01} \\ \tilde{M}_{01}^T & \tilde{M}_{11} \end{bmatrix}$$

also,

$$\tilde{C} = \tilde{L}^T \bar{C} \tilde{L}$$
$$\tilde{K} = \tilde{L}^T \bar{K} \tilde{L}$$

After transformation, the nonlinear terms in the inertia matrix $\bar{M}$ are localized and confined in the left-upper block $\tilde{M}_{00}$ which is associated with the motion of the rigid body only.

Now partition equation (18) into two equations. One equation corresponds to the rigid body motions with nonlinear terms in the inertia matrix whereas the other equation represents flexural vibrations in which the nonlinear terms appear in the right hand side of the equation and are treated as nonlinear forces. The partitioned equations provide

$$\tilde{M}_{00}\,\ddot{\gamma}_0 + \tilde{M}_{01}\,\ddot{\gamma}_1 + \tilde{C}_{00}\,\dot{\gamma}_0 + \tilde{C}_{01}\,\dot{\gamma}_1 + \tilde{K}_{00}\,\gamma_0 + \tilde{K}_{01}\,\gamma_1 = B_0 E_a + \tilde{f}_0 \tag{19}$$

$$\tilde{M}_{01}^T\,\ddot{\gamma}_0 + \tilde{M}_{11}\,\ddot{\gamma}_1 + \tilde{C}_{01}^T\,\dot{\gamma}_0 + \tilde{C}_{11}\,\dot{\gamma}_1 + \tilde{K}_{01}^T\,\gamma_0 + \tilde{K}_{11}\,\gamma_1 = \tilde{L}_{01}^T B_0 E_a + \tilde{f}_1 \tag{20}$$

where γ_0 represents the rigid body state vector with the appropriate dimension, γ_1 is the remaining flexible generalized coordinate, $\tilde{f}_0$ and $\tilde{f}_1$ denote the vectors of $\tilde{L}^T f(\eta,\dot{\eta})$, and $\tilde{M}_{ij}$, $\tilde{C}_{ij}$, $\tilde{K}_{ij}$, L_{ij} and B_i ($i = 0, 1$ & $j = 0,1$) are submatrices of $\tilde{M}$, $\tilde{C}$, $\tilde{K}$, $\tilde{L}$ and B respectively. Again recall that $\tilde{M}_{00}$ is the only submatrix containing the nonlinear functions associated with the state variables.

Now, a feedback linearization approach [7] is used to linearize the nonlinear terms in $\tilde{M}_{00}$ of equation (19), which is shown in the sequel. Replacing $\ddot{\gamma}_1$ in equation (19) with the one derived in equation (20) yields

$$[\tilde{M}_{00}-\tilde{M}_{01}\tilde{M}_{11}^{-1}\tilde{M}_{01}^{T}]\ddot{\gamma}_0 + [\tilde{C}_{00}-\tilde{M}_{01}\tilde{M}_{11}^{-1}\tilde{C}_{01}^{T}]\dot{\gamma}_0 + [\tilde{K}_{00}-\tilde{M}_{01}\tilde{M}_{11}^{-1}\tilde{K}_{01}^{T}]\gamma_0$$
$$+ [\tilde{C}_{01}-\tilde{M}_{01}\tilde{M}_{11}^{-1}\tilde{C}_{11}]\dot{\gamma}_1 + [\tilde{K}_{01}-\tilde{M}_{01}\tilde{M}_{11}^{-1}\tilde{K}_{11}]\gamma_1 = \tilde{f}_0 - \tilde{M}_{01}\tilde{M}_{11}^{-1}\tilde{f}_1$$
$$+ [B_0-\tilde{M}_{01}\tilde{M}_{11}^{-1}\tilde{L}_{01}^{T}B_0]E_a(t) \qquad (21)$$

An appropriate input is introduced to force equation (21) into the form of

$$\hat{M}_{00}\ddot{\gamma}_0 + \hat{C}_{00}\dot{\gamma}_0 + \hat{C}_{01}\dot{\gamma}_1 + \hat{K}_{00}\gamma_0 + \hat{K}_{01}\gamma_1 = \hat{B}_0 U \qquad (22)$$

where U is a modified input vector with an appropriate dimension for feedback linearization process, $\hat{M}_{00}$ is equivalent to ($\tilde{M}_{00}-\tilde{M}_{01}\tilde{M}_{11}^{-1}\tilde{M}_{01}^{T}$) with the nonlinear terms being eliminated, and

$$\hat{C}_{00} = [\tilde{C}_{00}-\tilde{M}_{01}\tilde{M}_{11}^{-1}\tilde{C}_{01}^{T}]$$
$$\hat{C}_{01} = [\tilde{C}_{01}-\tilde{M}_{01}\tilde{M}_{11}^{-1}\tilde{C}_{11}]$$
$$\hat{K}_{00} = [\tilde{K}_{00}-\tilde{M}_{01}\tilde{M}_{11}^{-1}\tilde{K}_{01}^{T}]$$
$$\hat{K}_{01} = [\tilde{K}_{01}-\tilde{M}_{01}\tilde{M}_{11}^{-1}\tilde{K}_{11}]$$
$$\hat{B}_0 = [B_0-\tilde{M}_{01}\tilde{M}_{11}\tilde{L}_{01}^{T}B_0]$$

Equation (21) is identical to equation (22), if

$$E_a(t) = \hat{B}_0^{-1}\{\tilde{M}_e\hat{M}_{00}^{-1}[\hat{B}_0U(t) - \hat{C}_{00}\dot{\gamma}_0 - \hat{C}_{01}\dot{\gamma}_1 - \hat{K}_{00}\gamma_0 - \hat{K}_{01}\gamma_1]$$
$$+ \hat{C}_{00}\dot{\gamma}_0 + \hat{C}_{01}\dot{\gamma}_1 + \hat{K}_{00}\gamma_0 + \hat{K}_{01}\gamma_1 - (\tilde{f}_0 - \tilde{M}_{01}\tilde{M}_{11}^{-1}\tilde{f}_1)\} \qquad (23)$$

where $\tilde{M}_e = (\tilde{M}_{00} - \tilde{M}_{01}\tilde{M}_{11}^{-1}\tilde{M}_{01}^{T}) = \hat{M}_{00} + \hat{M}_e$ with the matrix $\hat{M}_e$ containing the nonlinear terms associated with the state variables. Arranging equation (23) produces that

$$E_a(t)=\hat{B}_0^{-1}\{\hat{B}_0U(t) - (\tilde{f}_0-\tilde{M}_{01}\tilde{M}_{11}^{-1}\tilde{f}_1) + \hat{M}_e\hat{M}_{00}^{-1}[\hat{B}_0U(t) - \hat{C}_{00}\dot{\gamma}_0$$
$$- \hat{C}_{01}\dot{\gamma}_1 - \hat{K}_{00}\gamma_0 - \hat{K}_{01}\gamma_1]\} \qquad (24)$$

which relates the modified input for feedback linearization process with the actual input. Substituting equation (24) for $E_a(t)$ into equation (20) yields

$$\tilde{M}_{01}^T \ddot{\gamma}_0 + \tilde{M}_{11} \ddot{\gamma}_1 + \tilde{C}_{01}^T \dot{\gamma}_0 + \tilde{C}_{11} \dot{\gamma}_1 + \tilde{K}_{01}^T \gamma_0 + \tilde{K}_{11} \gamma_1 = \tilde{L}_{01}^T B_0 U + f_N + \tilde{f}_1 \qquad (25)$$

where

$$f_N = \tilde{L}_{01}^T B_0 \hat{B}_0^{-1} \{ \hat{M}_e \hat{M}_{00}^{-1} [\hat{B}_0 U - \hat{C}_{00} \dot{\gamma}_0 - \hat{C}_{01} \dot{\gamma}_1 - \hat{K}_{00} \gamma_0 - \hat{K}_{01} \gamma_1] - (\tilde{f}_0 - \tilde{M}_{01} \tilde{M}_{11}^{-1} \tilde{f}_1) \}$$

Equations (22) and (25) can be combined to yield a standard second-order time invariant linear system by which a conventional first order equation in state space form is obtained.

Output Feedback Gains

Robust eigensystem placement [14] is used to provide two robust output feedback gains for the above flexible manipulators. Referring to the open-loop eigenvalues of the system and the desired system responses, the frequencies associated with the modes and the damping ratio are assigned as shown in Table 1 for the one-arm case and Table 2 for the articulated case. Note that the closed-loop modal frequencies are maintained as the open-loop ones. In order to quickly suppress the vibrations, the damping ratio of the first mode is specified around 15%. The damping ratio of the second mode is slightly changed to 0.5%. The real eigenvalues associated with rigid bodies are located between -1 and -4 to minimize response time with suitable control torques.

The output feedback gain matrices for the two manipulators are shown in Table 3. Because the gains for the modal velocity feedback are comparably small, they are deleted for practical implementation of the future experiment. Those gains are applied in equation (9) such that

$$E_a(t) = -G \begin{bmatrix} \xi \\ \dot{\xi} \end{bmatrix} \qquad (26)$$

Discussion of Results

Several numerical simulations are performed to demonstrate the feasibility of the above active control algorithms. The model parameters are listed in Table 4 including material properties of the cart and flexible arms, and the conversion factors of the actuators and sensors.

The one-arm manipulator dynamics is represented by two rigid body modes and two flexible modes. The first two modes represent the cart linear position and the rotational angle of the flexible arm relative to the coordinate system attached on the cart. The latter two modes represent the first two bending modes of a fixed-free cantilever beam. Two rotary potentiometers are used to measure the first two modes, whereas two strain gages are used to measure the strains as shown in Fig. 2a.

For the articulated manipulator, one more rigid body mode is introduced to describe the rotary angle of the forearm, which is measured relative to the local coordinate of the previous arm. Also, two flexible modes are used for the forearm and two strain gages are used to sense the strains along the forearm (Fig. 2b). Because of the hardware limitations, velocity feedbacks of the flexible modes are not available and their gains should be eliminated as shown in Table 3.

Based upon the linear portion of the equations (22) and (25), the feedback-linearized equations are applied to perform the control schemes. In equation (24), the actual inputs to the motors $E_a(t)$ are evaluated to remove the nonlinear inertia term on the left-hand side of equation (9). The full state feedback is required in this process of linearization.

For the case of one-arm flexible manipulator, one task is to move the cart from positive 1.5 meters to a reference origin while simultaneously rotating the arm from 60 degrees to zero degree. Figure 4 shows the cart displacement, the relative root angle of the arm, the root strain, the relative displacement of the tip and the required torques of control inputs for this desired task. Generally speaking, it takes about 4 sec for this controller to complete the task. For the case of articulated flexible manipulator, two tasks are specified which are shown in Fig. 5. The controller finishes both tasks within 8 seconds. The required control torques of each simulation are feasible for the actuators in the future experiment.

Concluding Remarks

The active control of the articulated flexible manipulator carried by a translational cart in the planar motion has been investigated. The nonlinear dynamic equations for the manipulator are derived. The time-variant inertia matrix is linearized without approximation by using a suitable feedback linearization approach. The first-order state equations are then generated for controller design.

To design a controller to move the manipulator in an attainable workspace while suppressing the bending vibration of the flexible arms simultaneously, a robust pole placement approach is employed. It leads to two reliable output feedback gains which not only meet the need of the position control strategy but

also provide the system robustness. Several computer simulations for the flexible manipulator are conducted to demonstrate the feasibility of the controller design. Experimental tests are suggested in order to verify the numerical results disscussed herein.

Acknowledgement

This work was sponsored by NASA Langley Research Center under Grant NAG-1-830.

Reference

[1] Book, W. J., "Feedback Control of Two Beam, Two Joint Systems with Distributed Flexibility," Trans. of ASME, Journal of Dynamic Systems, Measurement, and Control, Dec. 1975, pp.424-431.

[2] Book, W. J., "Analysis of Massless Elastic Chains with Sero Controlled Joints," Trans. of the ASME, Journal of Dynamic Systems, Measurement, and Control, Sept. 1979, Vol.101, pp.187-192.

[3] Rakhsha, F. and Goldenberg, A. A., "Dynamic Modelling of a Single-link Flexible Robot," IEEE Trans. on Automatic Control, 1985, pp.984-989.

[4] Hastings, G. G. and Book, W. J., "Verification of a Linear Dynamic Model for Flexible Robotic Manipulators," IEEE Trans. on Automatic Control, 1986, pp.1024-1029.

[5] Bejczy, A. K., "Robot Arm Dynamics and Control," Tech. Memo 33-669, Jet Propulsion Laboratory, Feb. 1974.

[6] Dwyer, T. A. W., III and Batten, A. L., "Exact Multiaxial Spacecraft Attitude Maneuvers with Torque Saturation," Proc. IEEE International Conf. on Robotics and Automation, ST. Louis, Mo, March 1985, pp.978-983.

[7] Ghaemmaghami, P. and Juang, J.-N., "A Controller Design for Multi-body Large Angle Maneuvers," Proc. of International Symposium on the Mathematics of Networks and Systems, Phoenix, Arizona, June 15-19, 1987.

[8] Timoshenko, S. P. and Goodier, J. N., Theory of Elasticity, Third Edition, McGraw-Hill Book Company, New York, N.Y.,1970.

[9] Bishop, R. E. D. and Johnson, D. C., The Mechanics of Vibration, Cambridge University Press, London, England, 1960.

[10] Meirovitch, L., Analytical Methods in Vibrations, Third Printing, MacMillan Company, New York, N.Y., 1971.

[11] Juang, J.-N., Horta, L. G. and Robertshaw, H. H., "A Slewing Control Experiment for Flexible Structures," Journal of Guidance, Control, and Dynamics, Vol.9, Sep.-Oct. 1986, pp.599-607.

[12] Freund, E. and Syrbe, M., "Control of Industrial Robots by Means of Microprocessors," Lecture Notes in Control and Information Sciences, 1977, Vol.2, pp.167-185.

[13] Tarn, T. J., Bejczy, A. K., Isidori, A. and Chen, Y., "Nonlinear Feedback in Robot Arm Control," Proc. of the 23rd IEEE Conference on Decision and Control, Las Vegas, Nevada, Dec.12-14, 1984, pp.736-751.

[14] Juang, J.-N., Lim, K. B. and Junkins, J. L., "Robust Eigensystem Assignment," AIAA Journal of Guidance, Control and Dynamics, to appear.

Table 1: Frequency (Hz) and damping ratio for the one-arm manipulator

Open-loop		Closed-loop	
ω°	ζ°	ω	ζ
0.0		1.5782	
0.0		1.5782	
9.0656		2.3333	
33.7940		2.3333	
4.4287	13.2867 %	4.3277	15.0 %
27.8106	1.9230 %	26.8212	0.5 %

Table 2: Frequency (Hz) and damping ratio for the articulated manipulator

Open-loop		Closed-loop	
ω°	ζ°	ω	ζ
0.0		2.0613	
0.0		2.0613	
0.0		2.1332	
6.8068		2.1332	
33.7053		3.1701	
34.1371		3.1701	
1.8509	24.0858 %	1.8299	17.0 %
6.3521	5.2401 %	6.3581	17.0 %
21.3261	2.2987 %	20.6098	0.5 %
35.3678	0.4767 %	35.1438	0.5 %

Table 3: Output feedback gains

---

(1) Gain for the one-arm manipulator:

$$G = \begin{bmatrix} -6.5560 & -1.0032 & -9.0686 & -5.7710 & 6.3015 & -1.3067 & 0 & 0 \\ -0.8985 & -0.9722 & -1.8692 & -0.0205 & -1.0264 & 2.4745 & 0 & 0 \end{bmatrix}$$

(2) Gain for the two-arm articulated manipulator:

$$G = \begin{bmatrix} -13.7232 & -2.1394 & 0.5658 & 3.3502 & 91.3450 & -27.7692 \\ -3.1973 & -3.9846 & -0.7586 & -0.3899 & 38.3708 & -7.8262 \\ -0.8363 & -1.1753 & -1.3848 & 2.2190 & 55.2495 & -7.1356 \end{bmatrix}$$

$$\begin{bmatrix} -170.2792 & 0.0711 & -3.9826 & -1.0462 & 0 & 0 & 0 & 0 \\ -31.8523 & -3.6552 & -0.5281 & -1.1671 & 0 & 0 & 0 & 0 \\ 3.0059 & -0.9948 & -1.2351 & 2.1654 & 0 & 0 & 0 & 0 \end{bmatrix}$$

Table 4: Model parameters

Motors:

(1) Cart motor:

K_{t_0}	= 0.0346	N.m/amp
K_{b_0}	= 0.0342	Volt-sec/rad
R_{a_0}	= 4	ohm
I_{m_0}	= 4.7×10^{-6}	Kg-m^2
N_{g_0}	= 210	

(2) Arm motor:

K_{t_1}	= 9.3×10^{-3}	N.m/amp
K_{b_1}	= 9.2×10^{-3}	N.m/amp
R_{a_1}	= 1.1	ohm
I_{m_1}	= 2.3×10^{-6}	Kg-m^2
N_{g_1}	= 210	
m_1	= 0.92	Kg

Steel beam:

L	= 1.0	m
EI	= 0.71	N-m^2
ρ	= 0.47916	Kg/m
h	= 0.041×10^{-2}	m

Rigid cart:

m_c	= 0.588	Kg

Appendix

For the one-arm flexible manipulator shown in Fig. 1, the kinetic energy T and the potential energy V for small bending amplitude can be expressed as

$$2T = m\dot{y}^2 + \int_0^L \rho[\ \dot{\bar{y}} + \dot{\theta}_1 \times \bar{x}_1 - \dot{\bar{y}}_1\ ].[\ \dot{\bar{y}} + \dot{\theta}_1 \times \bar{x}_1 - \dot{\bar{y}}_1\ ]\ dx_1 \qquad (A1)$$

$$2V = \int_0^L EI(\ y_{1,x_1x_1}\ )^2\ dx_1 \qquad (A2)$$

where $\bar{x}_1$ is a vector tangent to the longitudinal axis of the base of flexible arm.

Moreover, the distributed coordinates are expanded in an orthogonal basis of assumed mode shapes as

$$y_1(x_1,t) = \psi_1^T(x_1)\ q_1(t)\ ;\psi_1^T=(\psi_{11},\ldots,\psi_{1n_1})\ \text{and}\ q_1^T=(q_{11},\ldots,q_{1n_1}) \qquad (A3)$$

where $\psi_1(x_1)$ is a vector of assumed mode shapes relative to a spatial coordinates derived from the fixed-free cantilever beam's boundary condition problem, $q_1(t)$ are generalized coordinates [8-10], and n_1 is an appropriate number of assumed modes.

Inserting equation (A3) into equations (A1) and (A2) yields

$$2T = m\dot{y}^2 + I_1\dot{\theta}_1^2 + \rho L\dot{y}^2 + \sum_{i=1}^{n_1}\sum_{j=1}^{n_1} m_{1ij}\dot{q}_{1i}\dot{q}_{1j} + \rho L^2 c\theta_1\dot{\theta}_1\dot{y}$$
$$- 2\sum_{i=1}^{n_1} P_{1i}\dot{q}_{1i}\dot{\theta}_1 - 2c\theta_1\sum_{i=1}^{n} h_{1i}\dot{q}_{1i}\dot{y} \qquad (A4)$$

$$2V = \sum_{i=1}^{n_1}\sum_{j=1}^{n_1} K_{1ij}q_{1i}q_{1j} \qquad (A5)$$

where

$$I_1 = \int_0^L \rho x_1^2\ dx_1$$

$$m_{1ij} = \int_0^L \rho\psi_{1i}(x_1)\psi_{1j}(x_1)\ dx_1$$

$$P_{1i} = \int_0^L \rho x_1\psi_{1i}(x_1)\ dx_1$$

$$h_{1i} = \int_0^L \rho\psi_{1i}(x_1)\ dx_1$$

$$\kappa_{1ij} = \int_0^L EI\psi_{1i,x_1x_1}\psi_{1j,x_1x_1}\, dx_1 \qquad \text{for } i,j=1,2,\ldots,n_1$$

To simplify the state variables in the above equations, denote $\xi_0=y$, $\xi_1=\theta_1$, $\xi_{1+i}=q_{1i}$, for $i=1,2,\ldots,n_1$, $Q_0=\tau_0$, $Q_1=\tau_1$, $Q_{1+i}=0$, for $i=1,2,\ldots,n_1$. Via the Lagrange's equation of motion [10], we obtain

$$d[\ \partial T/\partial\dot{\xi}_i\ ]/dt - \partial T/\partial\xi_i + \partial V/\partial\xi_i = Q_i \qquad i=0,1,\ldots,n_1$$

This leads to the equations of motion as shown in equations (3)-(6).

Similarly, for the articulated manipulator shown in Fig. 3, the kinetic energy and the potential energy can be derived as

$$\begin{aligned} 2T = m\dot{y}^2 &+ \int_0^L \rho(\ \dot{\bar{y}} + \dot{\bar{\theta}}_1\times\bar{x}_1 - \dot{\bar{y}}_1\ )(\ \dot{\bar{y}} + \dot{\bar{\theta}}_1\times\bar{x}_1 - \dot{\bar{y}}_1\ )\, dx_1 \\ &+ \int_0^L \rho(\ \dot{\bar{y}} + \dot{\bar{\theta}}_1\times\bar{L} + \dot{\bar{\theta}}_2\times\bar{x}_2 - \dot{\bar{y}}_1(L) - \dot{\bar{y}}_2\ ) \\ &\qquad (\ \dot{\bar{y}} + \dot{\bar{\theta}}_1\times\bar{L} + \dot{\bar{\theta}}_2\times\bar{x}_2 - \dot{\bar{y}}_1(L) - \dot{\bar{y}}_2\ )\, dx_2 \end{aligned} \tag{A6}$$

$$2V = \int_0^L EI\{\ y_{1,x_1x_1}\}^2\, dx_1 + \int_0^L EI\{\ y_{2,x_2x_2}\}^2\, dx_2 \tag{A7}$$

Expanding equations (A6) and (A7) provides

$$\begin{aligned} 2T = m\dot{y}^2 &+ 4I_1\dot{\theta}_1^2 + I_2\dot{\theta}_2^2 + 2\rho L\dot{y}^2 + \sum_{i=1}^{n_1}\sum_{j=1}^{n_1} m_{1ij}\dot{q}_{1i}\dot{q}_{1j} \\ &+ \sum_{i=1}^{n_2}\sum_{j=1}^{n_2} m_{2ij}\dot{q}_{2i}\dot{q}_{2j} - 2\sum_{i=1}^{n_1} P_{1i}\dot{q}_{1i}\dot{\theta}_1 - 2\sum_{i=1}^{n_2} P_{2i}\dot{q}_{2i}\dot{\theta}_2 \\ &+ 3\rho L^2 c\theta_1\dot{\theta}_1\dot{y} - 2c\theta_1\sum_{i=1}^{n_1} h_{1i}\dot{q}_{1i}\dot{y} - 2c(\theta_1+\theta_2)\sum_{i=1}^{n_2} h_{2i}\dot{q}_{2i}\dot{y} \\ &+ \rho L\sum_{i=1}^{n_1}\sum_{j=1}^{n_1}\psi_{1i}(L)\psi_{1j}(L)\dot{q}_{1i}\dot{q}_{1j} + \rho L^2 c(\theta_1+\theta_2)\dot{y}\dot{\theta}_2 \\ &- 2\rho Lc\theta_1\sum_{i=1}^{n_1}\psi_{1i}(L)\dot{q}_{1i}\dot{y} + \rho L^3 c\theta_2\dot{\theta}_1\dot{\theta}_2 - 2\rho L^2\sum_{i=1}^{n_1}\psi_{1i}(L)\dot{q}_{1i}\dot{\theta}_1 \\ &- 2Lc\theta_2\sum_{i=1}^{n_2} h_{2i}\dot{q}_{2i}\dot{\theta}_1 - \rho L^2 c\theta_2\sum_{i=1}^{n_1}\psi_{1i}(L)\dot{q}_{1i}\dot{\theta}_2 \\ &+ 2c\theta_2\sum_{i=1}^{n_1}\sum_{j=1}^{n_2}\psi_{1i}(L)h_{2j}\dot{q}_{1i}\dot{q}_{2j} \end{aligned} \tag{A8}$$

$$2V = \sum_{i=1}^{n_1}\sum_{j=1}^{n_1} K_{1ij}q_{1i}q_{1j} + \sum_{i=1}^{n_2}\sum_{j=1}^{n_2} K_{2ij}q_{2i}q_{2j} \tag{A9}$$

where

$$I_1 = \int_0^L \rho x_1^2 \, dx_1$$

$$I_2 = \int_0^L \rho x_2^2 \, dx_2$$

$$m_{1ij} = \int_0^L \rho \psi_{1i}(x_1)\psi_{1j}(x_1) \, dx_1$$

$$m_{2ij} = \int_0^L \rho \psi_{2i}(x_2)\psi_{2j}(x_2) \, dx_2$$

$$P_{1i} = \int_0^L \rho x_1 \psi_{1i}(x_1) \, dx_1$$

$$P_{2i} = \int_0^L \rho x_2 \psi_{2i}(x_2) \, dx_2$$

$$h_{1i} = \int_0^L \rho \psi_{1i}(x_1) \, dx_1$$

$$h_{2i} = \int_0^L \rho \psi_{2i}(x_2) \, dx_2$$

$$K_{1ij} = \int_0^L EI\psi_{1i,x_1x_1}\psi_{1j,x_1x_1} \, dx_1$$

$$K_{2ij} = \int_0^L EI\psi_{2i,x_2x_2}\psi_{2j,x_2x_2} \, dx_2$$

where n_1 and n_2 are the numbers of the shape functions for the first arm and the forearm respectively.

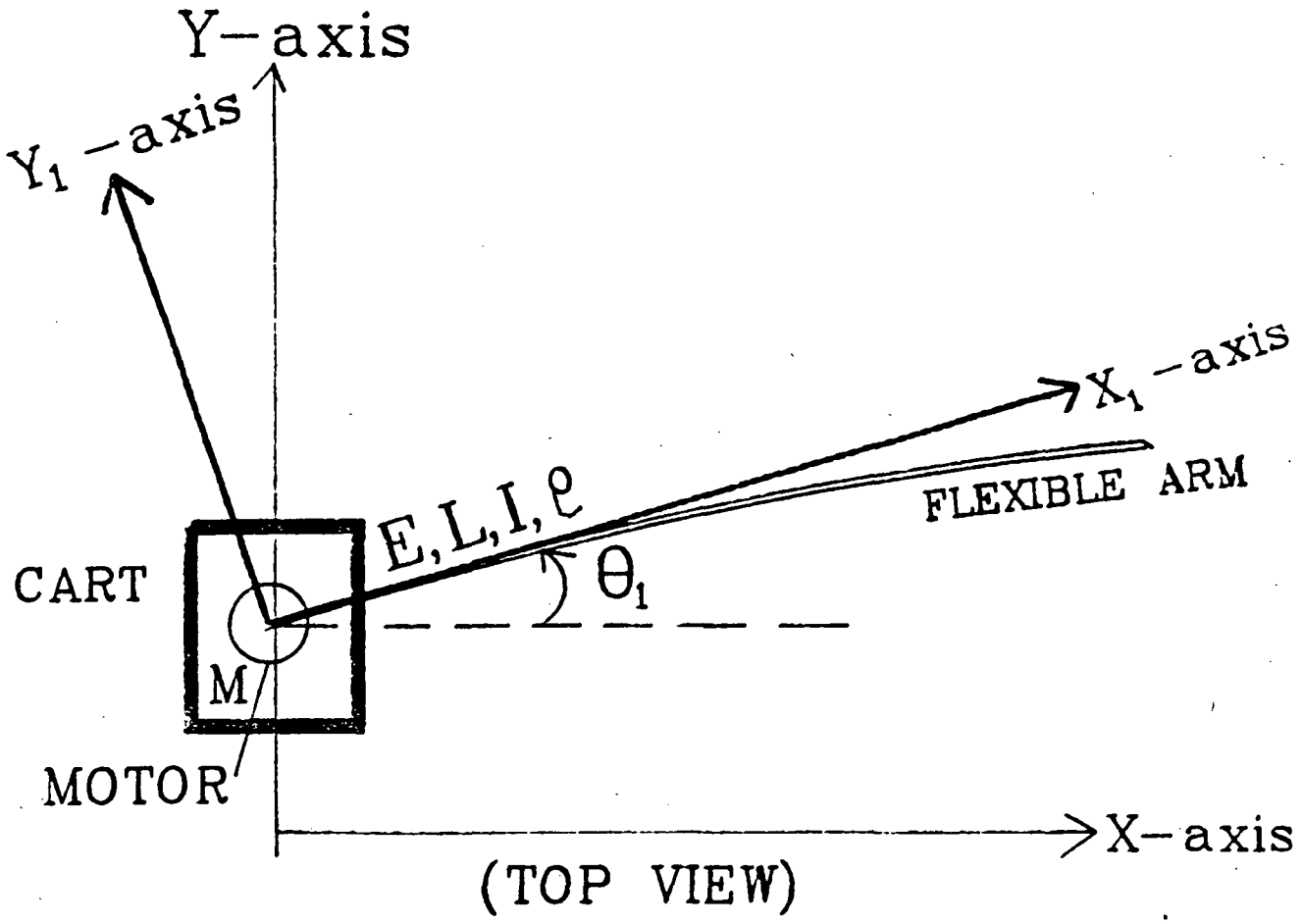

Figure 1: The coordinate system and notations of the cart and the flexible arm for the one-arm manipulator.

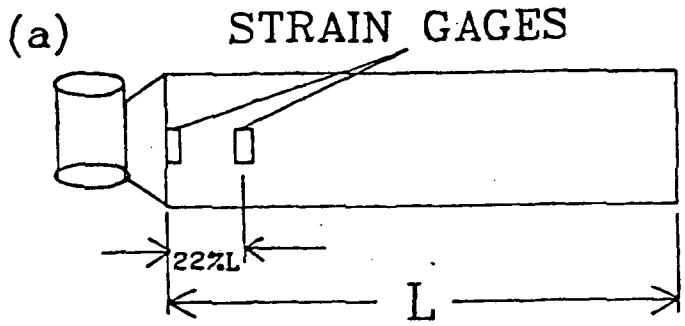

Figure 2a: Locations of the strain gages for the one-arm manipulator.

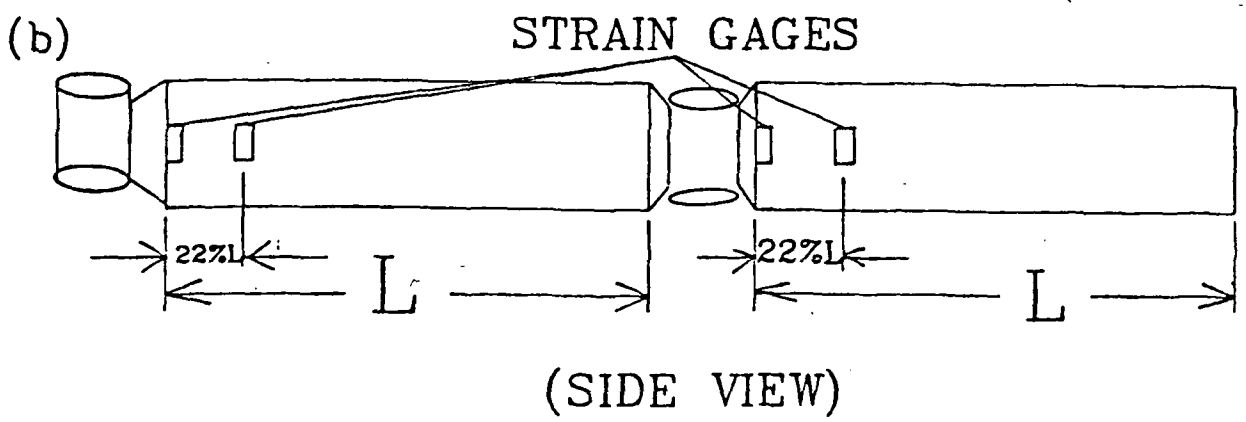

Figure 2b: Locations of the strain gages for the articulated manipulator.

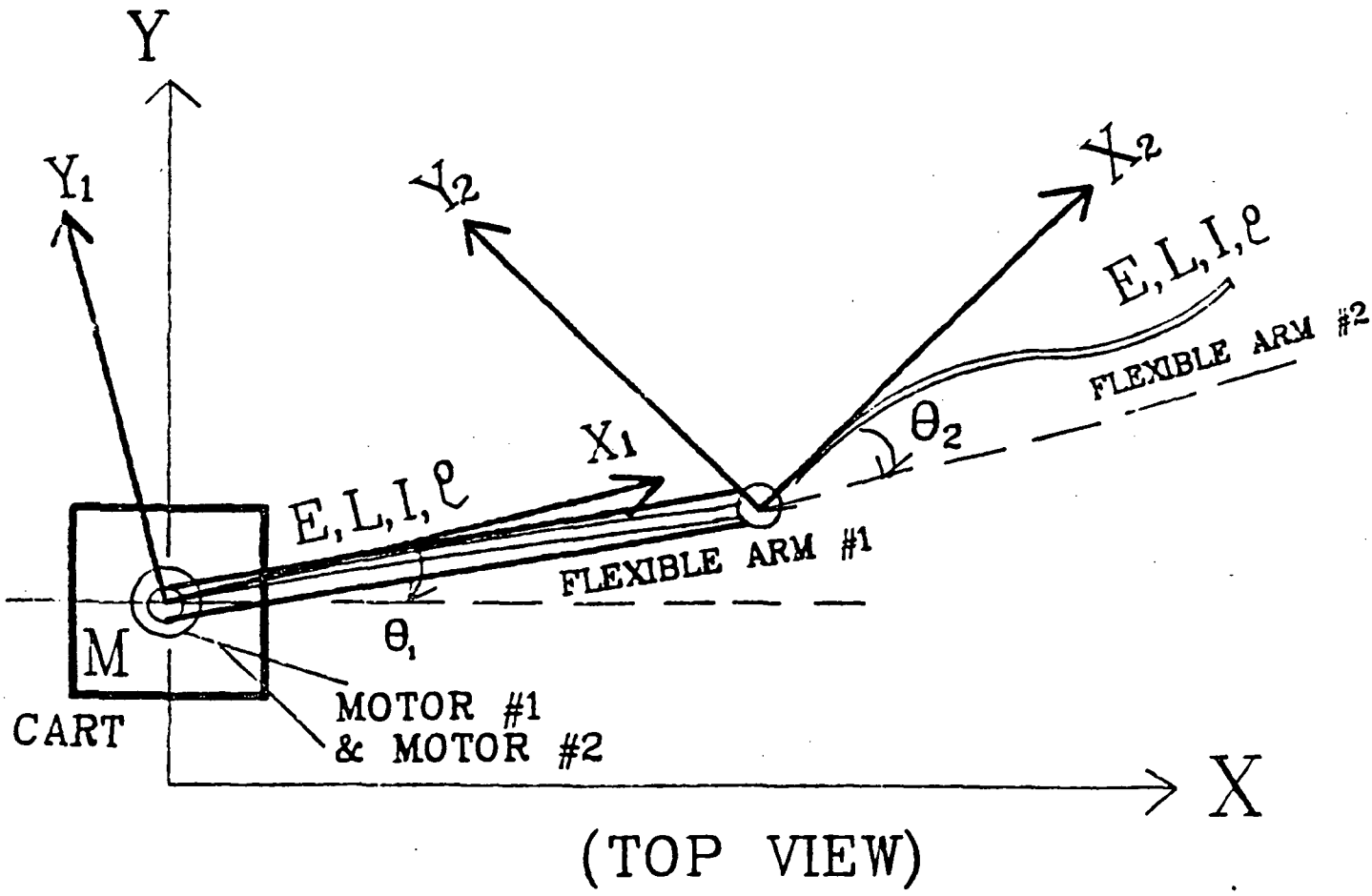

Figure 3: The coordinate system and notations of the cart and two arms for the articulated manipulator.

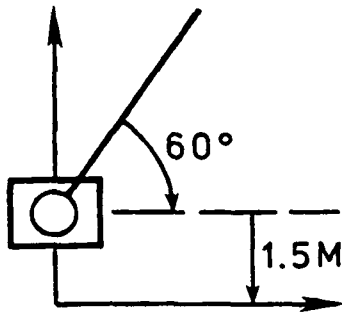

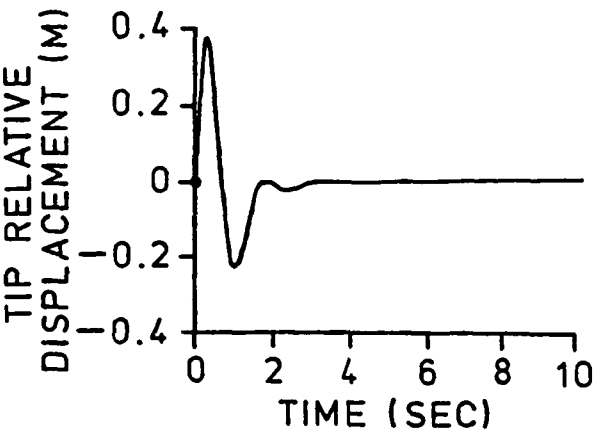

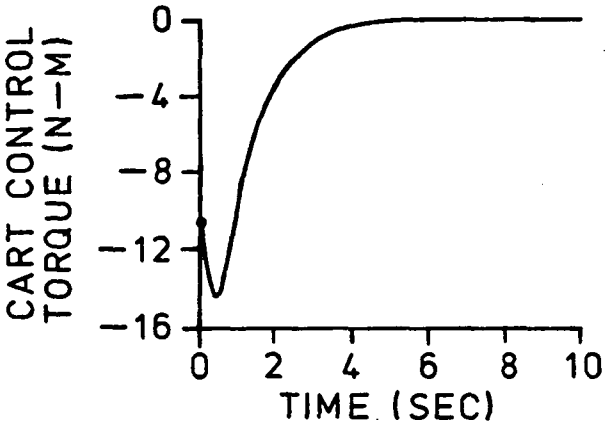

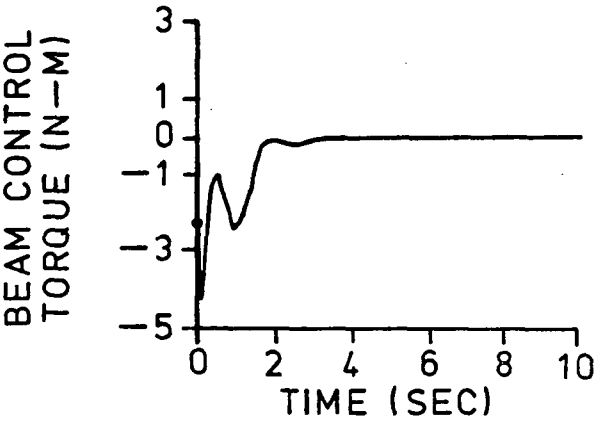

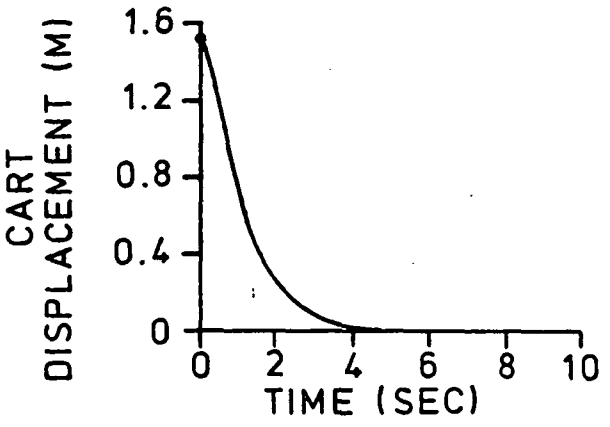

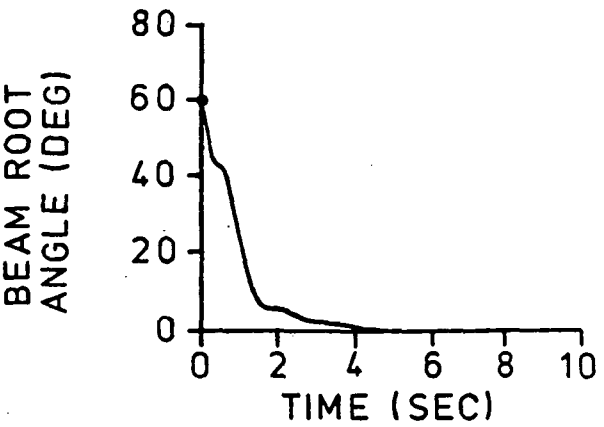

Figure 4: Numerical simulation of the one-arm manipulator; 1.5 m cart displacement and 60° manipulation.

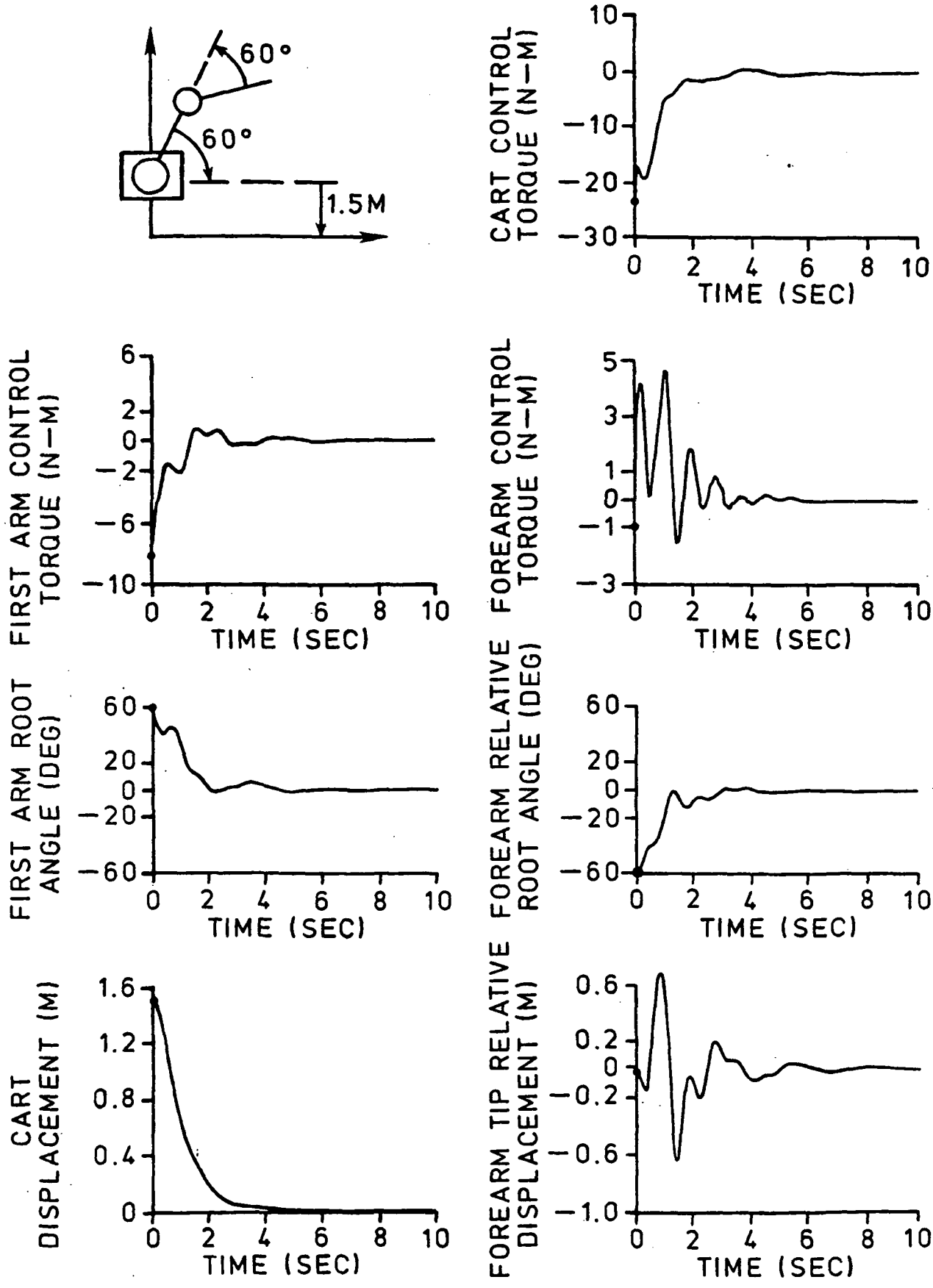

Figure 5a: Numerical simulation of the articulated manipulator; 1.5 m cart displacement, + 60° for the first arm and - 60° for the forearm manipulation.

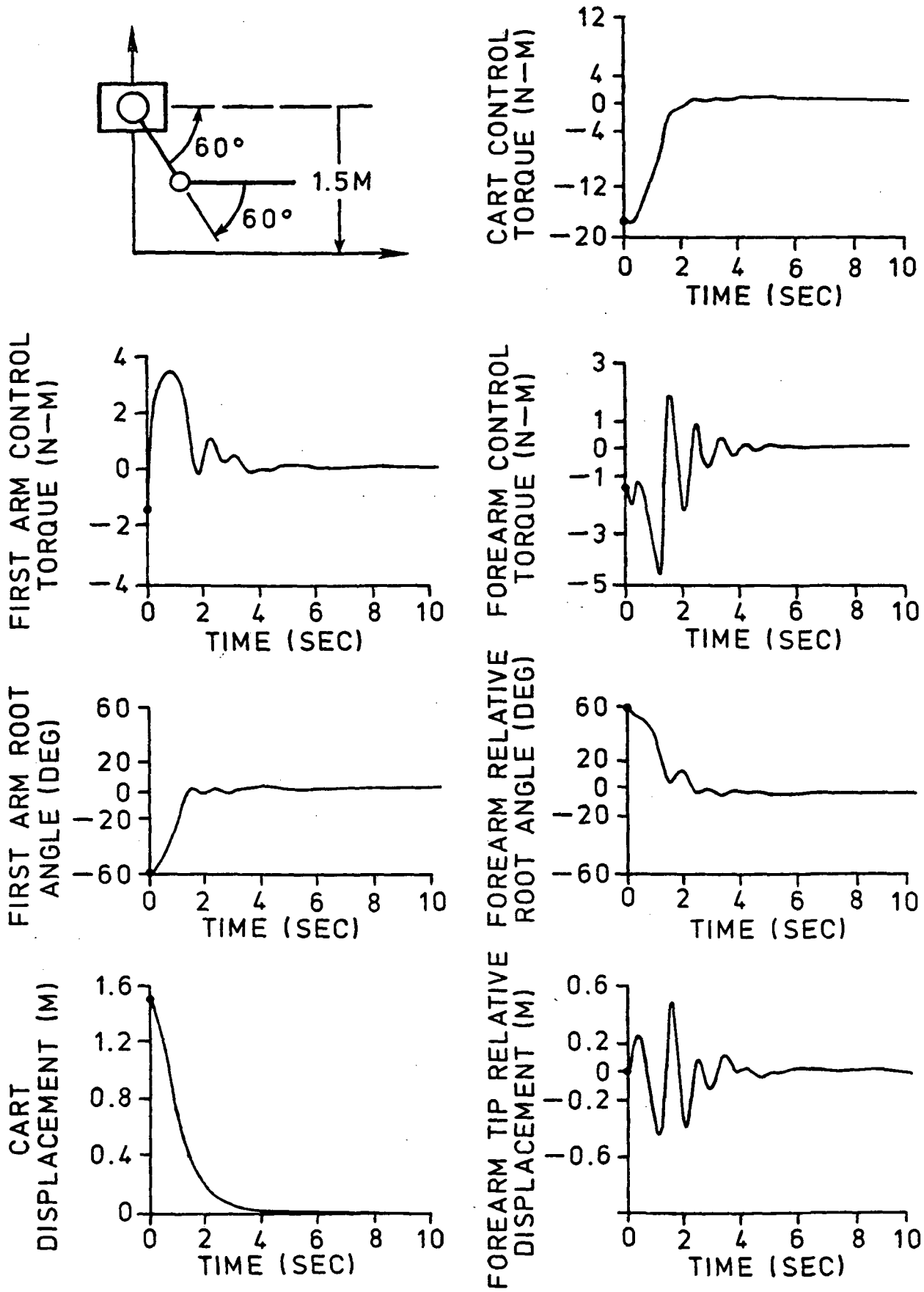

Figure 5b: Numerical simulation of articulated manipulator; 1.5 m cart displacement, - 60° for the first arm and + 60° for the forearm manipulation.